Progress In Electromagnetics Research, PIER 66, 51–63, 2006

ELECTROMAGNETIC SCATTERING BY MIXED CONDUCTING/DIELECTRIC OBJECTS USING HIGHER-ORDER MOM

S. G. Wang, X. P. Guan, D. W. Wang, X. Y. Ma, and Y. Su

School of Electronic Science and Technology
National University of Defense Technology
Changsha 410073, China

Abstract—In this paper, the higher order hierarchical basis functions are employed to solve the electric field integral equation for computing electromagnetic scattering from three-dimension bodies comprising both conducting and dielectric objects. In higher-order methods of moments (HO-MoM), the equivalent surface electric and magnetic currents are usually expanded by the same basis functions, which are not appropriate in our problem here. The pointwise orthogonal basis functions respectively for electric and magnetic currents are proposed in our improved HO-MoM. Quadrilateral patches are used in curvilinear geometry modeling since they result in the lowest number of unknowns. Numerical solution procedure is particularly analyzed, and numerical results are given for various structures and compared with other available data lastly.

1. INTRODUCTION

Electromagnetic scattering from composite bodies that consist of both conducting and dielectric objects is an important and challenging problem in the field of computation electromagnetics [1, 2]. It is more interested these years both in frequency [3–8] and time domains [9], especially for complex radar targets in real time. When the dielectric objects are homogenous or piecewise homogenous, on the bases of the equivalent principle, the method of moments (MoM) is preferred because the problem can be formulated in the terms of surface integrals over the conducting and dielectric surfaces at a few number of unknowns. However, the MoM usually results in a matrix of very large scale when applied to analyzing electrically large objects. Some fast algorithms, such as the multilevel fast multipole algorithm [3, 4], precorrected-FFT algorithm [5], and adaptive integral method [6, 7], are popularly employed to accelerate the matrix-vector manipulation. Otherwise, higher-order MoM (HO-MoM) can significantly reduce the number of unknowns, provide great flexibility and need less memory [10]. In this paper, a HO-MoM is improved to deal with this problem.

The higher order functions can be categorized as interpolatory or hierarchical. The interpolatory ones, as used in [4], require a mesh with equally sized elements due to the expansion order, while hierarchical bases combine the advantages of both low-order and higher order based into a single flexible basis [11, 12]. So the latter is applied in this paper with curvilinear geometry modeling by quadrilaterals.

For composite metallic and dielectric structures, if many junctions are considered [8, 13], the problem will be very complex. A simple approach is that several separate bodies are respectively processed and electric field integral equation is employed as the next part, where it will not be appropriate to expand the equivalent surface electric and magnetic currents by the same basis functions [2]. The pointwise orthogonal basis functions respectively for electric and magnetic currents are proposed in our improved HO-MoM. Then, numerical solution procedure is particularly analyzed in the part 3. Lastly, in part 4, numerical results are given for various structures and compared with other available data.

2. SURFACE INTEGRAL EQUATION

Consider the electromagnetic scattering by an arbitrary shaped 3D composite metallic and dielectric bodies illuminated by a plane wave as shown in Fig. 1. Although the bodies are shown distinct, this is not the general case. If the bodies are joined together, they are treated as two bodies with a layer of zero-thickness freespace separating them.

We employ the equivalence principle to split the original problem into two separate ones. The first one is where the fields are equivalent external to the body and the second one is where the fields are equivalent internal to the body.

For the problem valid external to the dielectric region, as shown in Fig. 2, the conductor and dielectric bodies are replaced by fictitious mathematical surfaces and the region is filled with the homogeneous material (μ_1, ε_1) of medium 1. The electric current on S_c is $\boldsymbol{J}_c$, while electric and magnetic currents on surface external to $S_d\,(S_d^+)$ are $\boldsymbol{J}_d$ and $\boldsymbol{M}_d$. The field inside the surface S_d and S_c is set to zero. By enforcing the continuity of the tangential electric field, the following

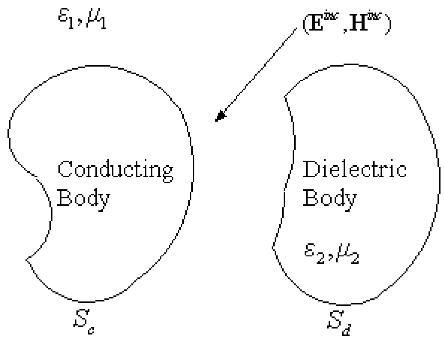

Figure 1. Arbitrary shaped conducting/dielectric body illuminated by a plne wave.

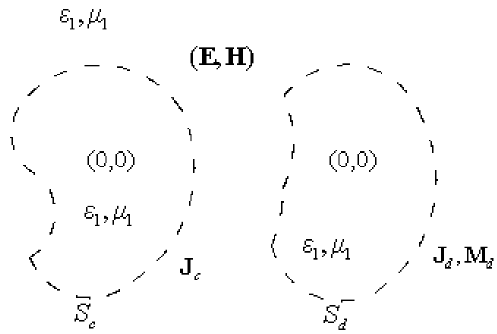

Figure 2. Equivalent problem outside.

equations are obtained:

$$\left[\boldsymbol{E}_c^{s1}(\boldsymbol{J}_c, \boldsymbol{J}_d, \boldsymbol{M}_d) + \boldsymbol{E}^{inc}\right]_{\tan} = 0, \quad \boldsymbol{r} \in S_c \tag{1}$$

$$\left[\boldsymbol{E}_d^{s1}(\boldsymbol{J}_c, \boldsymbol{J}_d, \boldsymbol{M}_d) + \boldsymbol{E}^{inc}\right]_{\tan} = 0, \quad \boldsymbol{r} \in S_d^+ \tag{2}$$

where the superscript 1 respresents the scattered field is computed in the medium 1.

For the second problem, the entire space is filled with the material of the dielectric medium (μ_2, ε_2) as shown in Fig. 3. The equivalent currents on surface internal to S_d (S_d^-) is $-\boldsymbol{J}_d$ and $-\boldsymbol{M}_d$. The electric field is zero outside S_d. By enforcing the continuity of the tangential electric field on S_d^-, the following integral equation may be derived:

$$\left[\boldsymbol{E}_d^{s2}(-\boldsymbol{J}_d, -\boldsymbol{M}_d)\right]_{\tan} = 0, \quad \boldsymbol{r} \in S_d^- \tag{3}$$

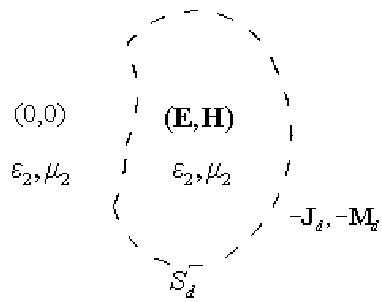

Figure 3. Equivalent problem inside.

where the superscript 2 represents the scattered field is computed in the medium 2.

3. NUMERICAL SOLUTION PROCEDURE USING HIGHER ORDER HIERATICAL BASIS FUNCTIONS

3.1. Curvilinear Geometry Modeling

In order to obtain a flexible algorithm that can be easily applied to different structures, it is desirable to perform the geometrical modeling by using only one specific simple class of isoparametric elements, e.g., bilinear surfaces. A bilinear surface is, in general, a nonplanar quadrilateral, which is defined uniquely by its four arbitrarily spaced vertices. The parametric equation of such an isoparametric element can be written in the form as [13]

$$\boldsymbol{r}(u,v) = \boldsymbol{r}_c + u\boldsymbol{r}_u + v\boldsymbol{r}_v + uv\boldsymbol{r}_{uv}, \quad -1 \leq u,\ v \leq 1 \tag{4}$$

where vectors $\boldsymbol{r}_c, \boldsymbol{r}_u, \boldsymbol{r}_v$, and $\boldsymbol{r}_{uv}$ are expressed as linear combinations of the vertex position vectors (A1)–(A4).

3.2. Pointwise Orthogonal Basis Functions

Consider a curved quadrilateral patch with an associated parametric curvilinear coordinate system defined by $-1 \leq u,\ v \leq 1$. The surface current density on each patch is represented as

$$\boldsymbol{J}(u,v) = \sum_{i=0}^{Nu}\sum_{j=0}^{Nv-1} \alpha_{uij}\boldsymbol{f}_{uij}(u,v) + \sum_{i=0}^{Nu-1}\sum_{j=0}^{Nv} \alpha_{vij}\boldsymbol{f}_{vij}(u,v) \tag{5}$$

where

$$\boldsymbol{f}_{uij}(u,v) = \frac{P_i(u)v^j}{J(u,v)}\boldsymbol{a}_u(u,v) \tag{6}$$

$$\boldsymbol{f}_{vij}(u,v) = \frac{u^i P_j(v)}{J(u,v)}\boldsymbol{a}_v(u,v) \tag{7}$$

$$J(u,v) = |\boldsymbol{a}_u(u,v) \times \boldsymbol{a}_v(u,v)|$$

$$P_i(u) = \begin{cases} 1-u, & i=0 \\ 1+u, & i=1 \\ u^i-1, & i \geq 2, \quad \text{even} \\ u^i-u, & i \geq 3, \quad \text{odd} \end{cases}$$

$$\boldsymbol{a}_u(u,v) = \frac{\partial \boldsymbol{r}(u,v)}{\partial u}, \ \boldsymbol{a}_v(u,v) = \frac{\partial \boldsymbol{r}(u,v)}{\partial v} \tag{8}$$

N_u and N_v are the adopted degrees of the polynomial current approximation, α_{uij} and α_{vij} are unknown coefficients. $\boldsymbol{a}_u$ and $\boldsymbol{a}_v$ are unitary vectors.

The basis functions for magnetic current $\boldsymbol{M}$ should be pointwise orthogonal to those for $\boldsymbol{J}$, in the form as

$$\boldsymbol{M}(u,v) = \sum_{i=0}^{Nu}\sum_{j=0}^{Nv-1} \beta_{uij}\boldsymbol{g}_{uij}(u,v) + \sum_{i=0}^{Nu-1}\sum_{j=0}^{Nv}\beta_{vij}\boldsymbol{g}_{vij}(u,v) \tag{9}$$

where

$$\boldsymbol{g}_{uij}(u,v) = \frac{P_i(u)v^j}{J(u,v)}\hat{\boldsymbol{n}}(u,v) \times \boldsymbol{a}_u(u,v) \tag{10}$$

$$\boldsymbol{g}_{vij}(u,v) = \frac{u^i P_j(v)}{J(u,v)}\hat{\boldsymbol{n}}(u,v) \times \boldsymbol{a}_v(u,v) \tag{11}$$

$$\hat{\boldsymbol{n}}(u,v) = \frac{\boldsymbol{a}_u(u,v) \times \boldsymbol{a}_v(u,v)}{J(u,v)} \tag{12}$$

β_{uij} and β_{vij} are unknown coefficients.

3.3. Matrix Element Evaluation

Using the potential theory, the scattered electric field $\boldsymbol{E}^s$ due to the electric current $\boldsymbol{J}$ and the magnetic current $\boldsymbol{M}$ may be written in terms of potential functions as [1]

$$\boldsymbol{E}^s(\boldsymbol{J},\boldsymbol{M}) = -j\omega \boldsymbol{A}(\boldsymbol{J}) - \nabla\Phi(\boldsymbol{J}) - \frac{1}{\varepsilon}\nabla \times \boldsymbol{F}(\boldsymbol{M}) \tag{13}$$

Without loss of generality, only u-directed components in testing and basis functions are considered in the following with the understanding that v-directed components can be obtained by interchanging u and v. We substitute (5), (9) into (13), take the testing functions the same as the basis functions of $\boldsymbol{J}$. The general expression for the MoM matrix elements is

$$Z_{pq} = Z'_{pq} + Z''_{pq} \tag{14}$$

$$Z'_{pq} = \left\langle \boldsymbol{f}_p^u, -j\omega \boldsymbol{A}(\boldsymbol{f}_q^u) \right\rangle + \left\langle \boldsymbol{f}_p^u, -\nabla\Phi(\boldsymbol{f}_q^u) \right\rangle \tag{15}$$

$$Z''_{pq} = \left\langle \boldsymbol{f}_p^u, -\frac{1}{\varepsilon}\nabla \times \boldsymbol{F}(\boldsymbol{g}_q^u) \right\rangle \tag{16}$$

where $\boldsymbol{f}_p^u$ is the u-directed component of the p'th testing function, and $\boldsymbol{f}_q^u$ is the u-directed component of the q'th basis function. Z'_{pq} can be written as linear combinations of the generic integral [12]

$$\xi^{uu}(i_m, j_m, i_n, j_n) = \int_{-1}^{1}\int_{-1}^{1}\int_{-1}^{1}\int_{-1}^{1} u_m^{i_m} v_m^{j_m} u_n^{i_n} v_n^{j_n} (\boldsymbol{a}_u^n \cdot \boldsymbol{a}_u^m) g(R) du_n dv_n du_m dv_m \tag{17}$$

where $g(R) = e^{-jkR}/(4\pi R)$ is the Green's function, and k is the wave number, $R = |\boldsymbol{r} - \boldsymbol{r}'|$ is the distance from the field point, $\boldsymbol{r}$, to the source point, $\boldsymbol{r}'$.

Let

$$I_1(i_m, j_m, i_n, j_n) = \int_{-1}^{1}\int_{-1}^{1}\int_{-1}^{1}\int_{-1}^{1} u_m^{i_m} v_m^{j_m} u_n^{i_n} v_n^{j_n} g(R) du_n dv_n du_m dv_m \tag{18}$$

and we have

$$\begin{aligned} \xi^{uu}(i_m, j_m, i_n, j_n) = {} & \boldsymbol{r}_u^m \cdot \boldsymbol{r}_u^n I_1(i_m, j_m, i_n, j_n) \\ & + \boldsymbol{r}_u^m \cdot \boldsymbol{r}_{uv}^n I_1(i_m, j_m, i_n, j_n + 1) \\ & + \boldsymbol{r}_{uv}^m \cdot \boldsymbol{r}_u^n I_1(i_m, j_m + 1, i_n, j_n) \\ & + \boldsymbol{r}_{uv}^m \cdot \boldsymbol{r}_{uv}^n I_1(i_m, j_m + 1, i_n, j_n + 1) \end{aligned} \tag{19}$$

when v-directed components in basis and testing functions are considered, (19) can be rewritten as (A5)–(A7).

Next, extracting the principle part of the curl term, we may rewrite (16) as

$$\left\langle \boldsymbol{f}_u^m, -\frac{1}{\varepsilon}\nabla \times \boldsymbol{F}(\boldsymbol{g}_u^n) \right\rangle = -\frac{1}{\varepsilon}\left\langle \boldsymbol{f}_u^m, \pm\frac{1}{2}\hat{\boldsymbol{n}}(u,v) \times \boldsymbol{g}_u^n \right\rangle - \frac{1}{\varepsilon}\left\langle \boldsymbol{f}_u^m, \nabla \times \tilde{\boldsymbol{F}}(\boldsymbol{g}_u^n) \right\rangle \tag{20}$$

where $\tilde{\boldsymbol{F}}$ represents $\boldsymbol{F}$ with singular term removed. And in the first inner product term of the right-hand side of (20), the positive sign is used when $\boldsymbol{r} \in S_d^+$, and negative sign otherwise.

Note (6) and (10), there may be

$$\left\langle \boldsymbol{f}_u^m, \pm\frac{1}{2}\hat{\boldsymbol{n}}(u_n, v_n)\times\boldsymbol{g}_u^n \right\rangle = \left\langle \boldsymbol{f}_u^m, \pm\frac{1}{2}\hat{\boldsymbol{n}}(u_n, v_n)\times(\hat{\boldsymbol{n}}(u_n, v_n)\times\boldsymbol{f}_u^n) \right\rangle = \mp\frac{1}{2}\left\langle \boldsymbol{f}_u^m, \boldsymbol{f}_u^n \right\rangle$$

Similarly, as (17)–(19), $\langle \boldsymbol{f}_u^m, \boldsymbol{f}_u^n \rangle$ may be written as linear combinations of (21).

$$\begin{aligned} \xi_2^{uu}(i_m, j_m, i_n, j_n) = \; & \boldsymbol{r}_u^m \cdot \boldsymbol{r}_u^n I_2(i_m, j_m, i_n, j_n) \\ & + \boldsymbol{r}_u^m \cdot \boldsymbol{r}_{uv}^n I_2(i_m, j_m, i_n, j_n + 1) \\ & + \boldsymbol{r}_{uv}^m \cdot \boldsymbol{r}_u^n I_2(i_m, j_m + 1, i_n, j_n) \\ & + \boldsymbol{r}_{uv}^m \cdot \boldsymbol{r}_{uv}^n I_2(i_m, j_m + 1, i_n, j_n + 1) \end{aligned} \tag{21}$$

where

$$I_2(i_m, j_m, i_n, j_n) = \int_{-1}^{1}\int_{-1}^{1}\int_{-1}^{1}\int_{-1}^{1} u_m^{i_m} v_m^{j_m} u_n^{i_n} v_n^{j_n} \frac{1}{J} du_n dv_n du_m dv_m \tag{22}$$

When v-directed components in basis and testing functions are considered, (21) can be respectively rewritten as (A8)–(A10).

The second inner product term of the right-hand side of (20) can be written as linear combinations of the generic integral

$$\begin{aligned} \xi_3^{uu}(i_m, j_m, i_n, j_n) = & \int_{-1}^{1}\int_{-1}^{1}\int_{-1}^{1}\int_{-1}^{1} u_m^{i_m} v_m^{j_m} u_n^{i_n} v_n^{j_n} \boldsymbol{a}_u^m \\ & \cdot \left[(\hat{\boldsymbol{n}}^n \times \cdot \boldsymbol{a}_u^n) \times \nabla' g(R) \right] du_n dv_n du_m dv_m \end{aligned} \tag{23}$$

Substituting (12) into (23), we obtain

$$\begin{aligned} \xi_3^{uu}(i_m, j_m, i_n, j_n) = & \int_{-1}^{1}\int_{-1}^{1}\int_{-1}^{1}\int_{-1}^{1} u_m^{i_m} v_m^{j_m} u_n^{i_n} v_n^{j_n} \boldsymbol{a}_u^m \\ & \cdot \left[((\boldsymbol{a}_u^n \times \boldsymbol{a}_v^n) \times \boldsymbol{a}_u^n) \times \frac{\nabla' g(R)}{J} \right] du_n dv_n du_m dv_m \end{aligned} \tag{24}$$

where $R \neq 0$. When v-directed components in basis and testing functions are considered, (24) can be respectively rewritten as (A11)–(A13).

(18), (22) and (24) may be computed using the Gauss-Legendre integration formulations or numerical annihilation procedure of self-term matrix elements. Then, matrix elements are evaluated.

4. NUMERICAL EXAMPLES

In this section, some numerical examples are presented to validate the implementation procedure and to demonstrate the accuracy of the present method. As all known, HO-MoM requires less memory and CPU time [8], so the taken memory and CPU time in the method are not shown here.

As a first example, we consider the electromagnetic scattering from a 0.5λ (λ is the wavelength in free space) dielectric cube of $\varepsilon_r = 2.0$ (the relative permittivity) covered by a conducting plate of dimension $0.5\lambda \times 0.5\lambda$. The conducting plate is placed on the top surface of the dielectric cube. The composite structure is illuminated by an x-polarized plane wave incident from the bottom ($\theta = 180°$). The conducting plate was divided into 16 quadrilaterals. The dielectric cube was approximated by 96 quadrilaterals. In our HO-MoM of this case, the order is $M = N_u = N_v = 1$. The bistatic RCS computed in the plane $\varphi = \pi$ is shown in Fig. 4. Very good agreement is observed between the traditional MoM of RWG basis functions solution and our method.

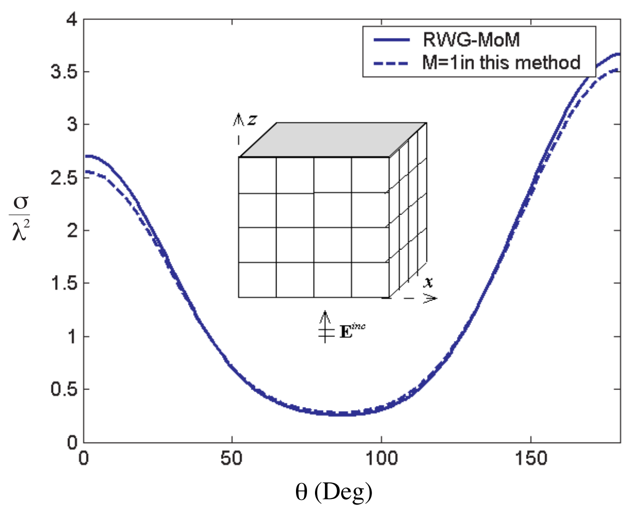

Figure 4. Bistatic RCS of a disk/cube structure.

As the second example consider the electromagnetic scattering from a conducting cylinder capped by a dielectric cone as shown in Fig. 5. The conducting cylinder has a diameter of 0.6λ and a height of 0.6λ. The conducting cylinder is capped by a dielectric cone of height 0.6λ and has the same diameter as that of the conducting cylinder. The

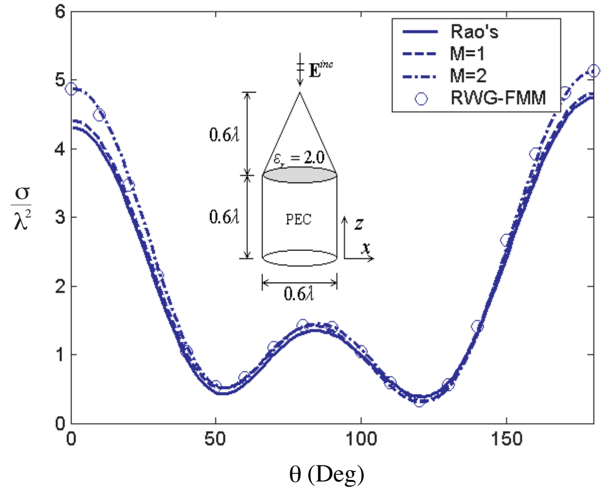

Figure 5. Bistatic RCS of a conducting cylinder/dielectric cone structure.

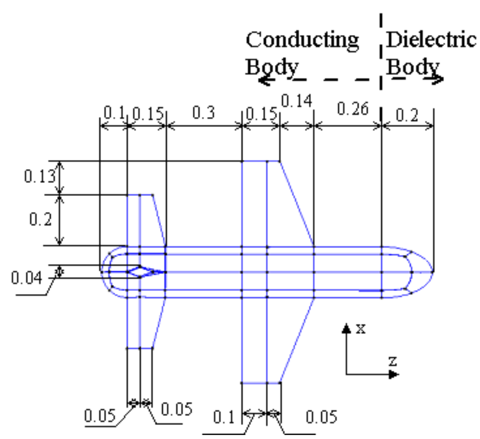

Figure 6a. The planform of the missle model.

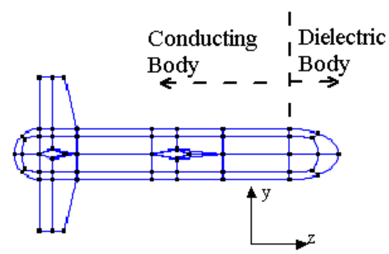

Figure 6b. The side view of the missle model.

dielectric constant for the cone is $\varepsilon_r = 2.0$. The structure is illuminated by a plane wave which is traveling from the tip of the dielectric cone toward the conducting cylinder. The dielectric cone and the conducting cylinder are modeled by 56 and 96 quadrilaterals. The bistatic RCS in the plane $\varphi = \pi$ with $M = 1$ and $M = 2$, which are compared with Rao's result [2] and those from fast multipole algorithm based on RWG

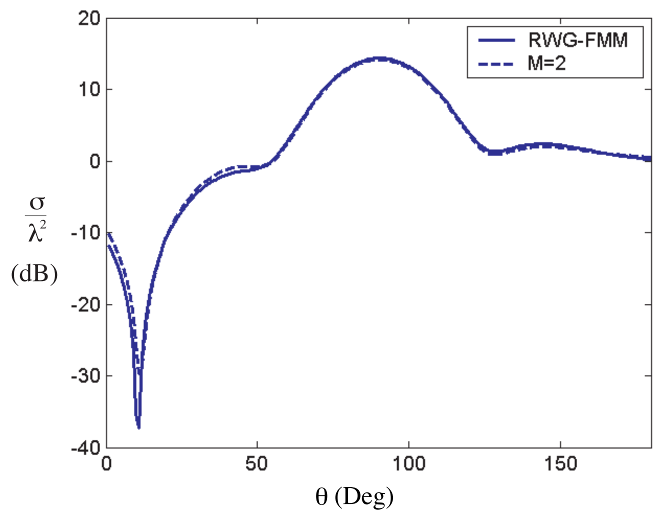

Figure 7. Bistatic RCS of the composite missile model.

basis functions (RWG-FMM), are plotted in Fig. 5. We can see that agreement is reasonable.

The last example is a complex radar target, a kind of missile model, as shown in Figure 6a and Figure 6b. The unit of labels is meter (m). The main part is a circle cylinder. The front part is half a spheroids, and the tail is half a sphere. The head is dielectric of the material $\varepsilon_r = 2.0$, and other parts are conducting structures. The incident wave is z-polarized and y-traveling with frequency $f = 0.6\,\text{GHz}$. The dielectric head and the conducting body are modeled by 64 and 472 quadrilaterals. The bastatic RCS of our method in the plane $\varphi = -0.5\pi$ with $M = 2$ and the result from RWG-FMM are shown in Fig. 7.

5. CONCLUSIONS

In this work, the higher order hieratical basis functions in HO-MoM are extended to solve the electric field integral equation for computing electromagnetic scattering from three-dimension bodies comprising both conducting and dielectric objects. The pointwise orthogonal basis functions are proposed and the numerical procedure is particularly analyzed. Several numerical results are presented to demonstrate the accuracy of the method.

APPENDIX A.

A.1. Constant Vectors in (4)

Suppose the vertex position vectors of a bilinear patch is respectively $\boldsymbol{r}_1, \boldsymbol{r}_2, \boldsymbol{r}_3$, and $\boldsymbol{r}_4$ in turn. The vectors in parametric equation can be written as

$$\boldsymbol{r}_c = 0.25(\boldsymbol{r}_1 + \boldsymbol{r}_2 + \boldsymbol{r}_3 + \boldsymbol{r}_4) \quad \text{(A1)}$$

$$\boldsymbol{r}_u = 0.25(-\boldsymbol{r}_1 - \boldsymbol{r}_2 + \boldsymbol{r}_3 + \boldsymbol{r}_4) \quad \text{(A2)}$$

$$\boldsymbol{r}_v = 0.25(-\boldsymbol{r}_1 + \boldsymbol{r}_2 + \boldsymbol{r}_3 - \boldsymbol{r}_4) \quad \text{(A3)}$$

$$\boldsymbol{r}_{uv} = 0.25(\boldsymbol{r}_1 - \boldsymbol{r}_2 + \boldsymbol{r}_3 - \boldsymbol{r}_4) \quad \text{(A4)}$$

A.2. Other Integrations Similar to (19)

When v-directed components in basis and testing functions are considered, (19) can be rewritten as

$$\begin{aligned}\xi^{uv}(i_m, j_m, i_n, j_n) = &\ \boldsymbol{r}_u^m \cdot \boldsymbol{r}_v^n I(i_m, j_m, i_n, j_n) \\ &+\boldsymbol{r}_u^m \cdot \boldsymbol{r}_{uv}^n I(i_m, j_m, i_n + 1, j_n) \\ &+\boldsymbol{r}_{uv}^m \cdot \boldsymbol{r}_v^n I(i_m, j_m + 1, i_n, j_n) \\ &+\boldsymbol{r}_{uv}^m \cdot \boldsymbol{r}_{uv}^n I(i_m, j_m + 1, i_n + 1, j_n) \quad \text{(A5)}\end{aligned}$$

$$\begin{aligned}\xi^{vu}(i_m, j_m, i_n, j_n) = &\ \boldsymbol{r}_v^m \cdot \boldsymbol{r}_u^n I(i_m, j_m, i_n, j_n) \\ &+\boldsymbol{r}_v^m \cdot \boldsymbol{r}_{uv}^n I(i_m, j_m, i_n, j_n + 1) \\ &+\boldsymbol{r}_{uv}^m \cdot \boldsymbol{r}_u^n I(i_m + 1, j_m, i_n, j_n) \\ &+\boldsymbol{r}_{uv}^m \cdot \boldsymbol{r}_{uv}^n I(i_m + 1, j_m, i_n, j_n + 1) \quad \text{(A6)}\end{aligned}$$

$$\begin{aligned}\xi^{vv}(i_m, j_m, i_n, j_n) = &\ \boldsymbol{r}_v^m \cdot \boldsymbol{r}_v^n I(i_m, j_m, i_n, j_n) \\ &+\boldsymbol{r}_v^m \cdot \boldsymbol{r}_{uv}^n I(i_m, j_m, i_n + 1, j_n) \\ &+\boldsymbol{r}_{uv}^m \cdot \boldsymbol{r}_v^n I(i_m + 1, j_m, i_n, j_n) \\ &+\boldsymbol{r}_{uv}^m \cdot \boldsymbol{r}_{uv}^n I(i_m + 1, j_m, i_n + 1, j_n) \quad \text{(A7)}\end{aligned}$$

A.3. Other Integrations Similar to (21)

When v-directed components in basis and testing functions are considered, (21) can be rewritten as

$$\begin{aligned}\xi_2^{uv}(i_m, j_m, i_n, j_n) = &\ \boldsymbol{r}_u^m \cdot \boldsymbol{r}_v^n I_2(i_m, j_m, i_n, j_n) \\ &+\boldsymbol{r}_u^m \cdot \boldsymbol{r}_{uv}^n I_2(i_m, j_m, i_n + 1, j_n) \\ &+\boldsymbol{r}_{uv}^m \cdot \boldsymbol{r}_v^n I_2(i_m, j_m + 1, i_n, j_n) \\ &+\boldsymbol{r}_{uv}^m \cdot \boldsymbol{r}_{uv}^n I_2(i_m, j_m + 1, i_n + 1, j_n) \quad \text{(A8)}\end{aligned}$$

$$\begin{aligned}\xi_2^{vu}(i_m,j_m,i_n,j_n) &= \boldsymbol{r}_v^m\cdot\boldsymbol{r}_u^n I_2(i_m,j_m,i_n,j_n)\\&+\boldsymbol{r}_v^m\cdot\boldsymbol{r}_{uv}^n I_2(i_m,j_m,i_n,j_n+1)\\&+\boldsymbol{r}_{uv}^m\cdot\boldsymbol{r}_u^n I_2(i_m+1,j_m,i_n,j_n)\\&+\boldsymbol{r}_{uv}^m\cdot\boldsymbol{r}_{uv}^n I_2(i_m+1,j_m,i_n,j_n+1)\end{aligned}\tag{A9}$$

$$\begin{aligned}\xi_2^{vv}(i_m,j_m,i_n,j_n) &= \boldsymbol{r}_v^m\cdot\boldsymbol{r}_v^n I_2(i_m,j_m,i_n,j_n)\\&+\boldsymbol{r}_v^m\cdot\boldsymbol{r}_{uv}^n I_2(i_m,j_m,i_n+1,j_n)\\&+\boldsymbol{r}_{uv}^m\cdot\boldsymbol{r}_v^n I_2(i_m+1,j_m,i_n,j_n)\\&+\boldsymbol{r}_{uv}^m\cdot\boldsymbol{r}_{uv}^n I_2(i_m+1,j_m,i_n+1,j_n)\end{aligned}\tag{A10}$$

A.4. Other Integrations Similar to (24)

When v-directed components in basis and testing functions are considered, (24) can be rewritten as

$$\begin{aligned}\xi_3^{uv}(i_m,j_m,i_n,j_n) &= \int_{-1}^{1}\int_{-1}^{1}\int_{-1}^{1}\int_{-1}^{1} u_m^{i_m}v_m^{j_m}u_n^{i_n}v_n^{j_n}\boldsymbol{a}_u^m\\&\cdot\left[((\boldsymbol{a}_u^n\times\boldsymbol{a}_v^n)\times\boldsymbol{a}_v^n)\times\frac{\nabla' g(R)}{J}\right]du_n dv_n du_m dv_m\end{aligned}\tag{A11}$$

$$\begin{aligned}\xi_3^{vu}(i_m,j_m,i_n,j_n) &= \int_{-1}^{1}\int_{-1}^{1}\int_{-1}^{1}\int_{-1}^{1} u_m^{i_m}v_m^{j_m}u_n^{i_n}v_n^{j_n}\boldsymbol{a}_v^m\\&\cdot\left[((\boldsymbol{a}_u^n\times\boldsymbol{a}_v^n)\times\boldsymbol{a}_u^n)\times\frac{\nabla' g(R)}{J}\right]du_n dv_n du_m dv_m\end{aligned}\tag{A12}$$

$$\begin{aligned}\xi_3^{vv}(i_m,j_m,i_n,j_n) &= \int_{-1}^{1}\int_{-1}^{1}\int_{-1}^{1}\int_{-1}^{1} u_m^{i_m}v_m^{j_m}u_n^{i_n}v_n^{j_n}\boldsymbol{a}_v^m\\&\cdot\left[((\boldsymbol{a}_u^n\times\boldsymbol{a}_v^n)\times\boldsymbol{a}_v^n)\times\frac{\nabla' g(R)}{J}\right]du_n dv_n du_m dv_m\end{aligned}\tag{A13}$$

REFERENCES

1. Sarkar, T. K., S. M. Rao, and A. R. Djordjevic, "Electromagnetic scattering and radiation from finite microstrip structures," *IEEE Trans. Antennas Propagat.*, Vol. 38, No. 11, 1568–1575, Nov. 1990.
2. Rao, S. M., T. K. Sarkar, P. Midya, and A. R. Djordjevic, "Electromagnetic radiation and scattering from finite conducting and dielectric structure: surface/surface formulation," *IEEE Trans. Antennas Propagat.*, Vol. 39, No. 7, 1034–1037, Nov. 1991.
3. Li, J.-Y. and L.-W. Li, "Electromagnetic scattering by a mixture of conducting and dielectric objects: analysis using method of

moments," *IEEE Trans. on Vehicular Technology*, Vol. 53, No. 2, 514–520, Mar. 2004.

4. Donepudi, K. C., J.-M. Jin, and W. C. Chew, "A higher order multilevel fast multipole algorithm for scattering from mixed conducting/dielectric bodies," *IEEE Trans. Antennas Propagat.*, Vol. 51, No. 10, 2814–2821, Oct. 2003.
5. Yuan, N., T. S. Yeo, X. C. Nie, L. W. Li, and Y. B. Gan, "Analysis of scattering from composite conducting and dielectric targets using the precorrected-FFT algorithm," *J. of Electromagn. Waves and Appl.*, Vol. 17, No. 3, 499–515, 2003.
6. Ewe, W.-B., L.-W. Li, and M.-S. Leong, "Solving mixed dielectric/conducting scattering problem using adaptive integral method," *Progress In Electromagnetics Research*, PIER 46, 143–163, 2004.
7. Nie, X.-C., N. Yuan, L.-W. Li, Y.-B. Gan, and T. S. Yeo, "A fast volume-surface integral equation solver for scattering from composite conducting-dielectric objects," *IEEE Trans. Antennas Propagat.*, Vol. 53, No. 2, 818–824, Oct. 2005.
8. Yla-Oijala, P., M. Taskiene, and J. Sarvas, "Surface integral equation method for general composite metallic and dielectric structures with junctions," *Progress In Electromagnetics Research*, PIER 52, 81–108, 2005.
9. Sarkar, T. K., W. Lee, and S. M. Rao, "Analysis of transient scattering from composite arbitrarily shaped complex structures," *IEEE Trans. Antennas Propagat.*, Vol. 48, No. 10, 1625–1634, Oct. 2000.
10. Jørgensen, E., J. L. Volakis, P. Meincke, and O. Breinbjerg, "Higher order hierarchical discretization scheme for surface integral equations for layered media," *IEEE Trans. Geosci Remote Sensing*, Vol. 42, 764–772, April 2004.
11. Jørgensen, E., J. L. Volakis, P. Meincke, and O. Breinbjerg, "Higher order hierarchical legendre basis functions for electromagnetic modeling," *IEEE Trans. Antennas Propagat.*, Vol. 52, 2985–2995, Nov. 2004.
12. Djordjevic, I. and B. M. Notaroš, "Double higher order method of moments for surface integral equation modeling of metallic and dielectric antennas and scatters," *IEEE Trans. Antennas Propagat.*, Vol. 52, 2118–2129, Aug. 2004.
13. Kolundzija, B. M., "Electromagnetic modeling of composite metallic and dielectric structures," *IEEE Trans. Microwave Theory Tech.*, Vol. 47, No. 7, 1021–1032, July 1999.